https://doi.org/10.30799/jnst.143.18040501 J. Nanosci. Tech. - Volume 4 Issue 5 (2018) 461–466

Share Your Innovations through JACS Directory

Journal of Nanoscience and Technology

Visit Journal at http://www.jacsdirectory.com/jnst

ISSN: 2455-0191

# Influence of Co-Dopant on Structural, Optical and Electrochemical Properties of Zinc Sulphide Quantum Dots

S. Velusubhash[1,*], K. Kalirajan[2], S. Harikengaram[3], R. Vettumperumal[4], R. Murugesan[5], A. Rajarajeswari[5]

[1]*Research Scholar (Reg. No. 9074), PG and Research Department of Chemistry, Sri Paramakalyani College, Alwarkurichi, Affiliated to Manonmaniam Sundaranar University, Abishekapatti, Tirunelveli – 627 012, Tamil Nadu, India.*
[2]*PG and Research Department of Chemistry, Sri Paramakalyani College, Alwarkurichi, Tirunelveli – 627 412, Tamil Nadu, India.*
[3]*PG Department of Chemistry, Pasumpon Muthuramalinga Thevar College, Melaneelithanallur, Tirunelveli – 627 953, Tamil Nadu, India.*
[4]*Department of Physics, V V College of Engineering, Tisaiyanvilai, Tirunelveli – 627 657, Tamil Nadu, India.*
[5]*Department of Chemistry, T.D.M.N.S. College, T. Kallikulam, Tirunelveli – 627 113, Tamil Nadu, India.*

ARTICLEDETAILS

*Article history:*
Received 11 July 2018
Accepted 25 July 2018
Available online 04 August 2018

*Keywords:*
Co-Precipitation
Quantum Dots
Band Gap
Photoluminescence
Photo Generated Electrons

ABSTRACT

In the present work, solution based simple chemical precipitation method has been employed to prepare undoped, cobalt (Co)-doped and cobalt, nickel (Co, Ni) co-doped ZnS quantum dots (QDs). The XRD pattern revealed that all samples displayed cubic zinc blende structure. The average crystallite size of as prepared ZnS QDs were found to be in 1.0 to 1.4 nm range. Surface morphological of synthesized samples were recorded and some distinction in morphological features between undoped, doped and co-doped ZnS QDs were noticed. EDX analysis confirms the presence of all corresponding elements in the samples. The blue-shift in the absorption spectra was observed. The optical band gap energy ($E_g$) for all the hybrid ZnS QDs samples were evaluated by using UV-Visible optical absorption spectral data. In PL analysis, emission band at 660 nm was found to be quenched as ZnS QDs interact with dopant and co-dopant. Electrochemical analysis was carried out by transition of photogenerated electrons in undoped, cobalt (Co)-doped and cobalt, nickel (Co, Ni) co-doped ZnS QDs modified glassy carbon electrodes. To authenticate the results of PL and electrochemical studies, photocatalytic behaviour of QDs were studied and positive impact of doping and co-doping process on photo degradation were noticed and discussed.

## 1. Introduction

Almost all materials classification including metals, insulators and semiconductors show size dependent electronic or optical properties in the quantum size system. Among these, semiconductors are the most excellent material showing appreciable modification in the optical and electronic properties through the alteration in the energy band gap via doping with other foreign metals. Recently semiconducting nanocrystalline materials have immensely attracted the interest in electronics and photonics application [1] such as light emitting diodes [2], photonics [3], chemical, biological and UV sensors [4], phosphors in displays and also in biomedical applications for biological labelling [5], diagnostics [6].

Among the various types of semiconductor nanostructures, zinc sulphide (ZnS) quantum dots have been considerably studied because of their size or shape dependent electronic and optical properties [7-9], which is also dependent on quantum confinement effects. Nano-structured ZnS exhibits excellent optical and electronic performances, which differ from the bulk ZnS material due to the three-dimensional electrons and holes confinement in a small volume [10]. ZnS is a wide band gap semiconductor material (Eg=3.6 eV). It is commercially used as a phosphor and also as thin-film electroluminescence devices [11, 12]. Semiconductor nanocrystals having dimensions smaller than 10 nm are also described as quantum dots [13].

Luminescence characteristics of metal ions impurity-activated ZnS nanocrystals differ markedly from those of the bulk undoped ZnS. The reasons for this behavior can be explained by two basic features. First, ZnS nanocrystallites are the high disperse nanocrystalline systems, i.e., the number of atoms on the surface are comparable to the number of those are located in the crystalline lattice itself. Physical and chemical properties, which are usually determined by the molecular structure of the bulk lattice, become increasingly dominated by the defect structure of surface and bulk. Second, the size-dependent properties of semiconductors ZnS nanocrystals are particularly interesting. The main contributions of metal doped and co-doped studies have demonstrated the size-dependent effect of the basic physical properties of the un-doped quantum dots. Quantum size effects (QSE) associated with the low dimension particles leads to numerous significant modifications in the physical properties of materials. These effects are prominent and lead to a discrete and size-dependent energy levels when the radius is fabricated less than the radius of Bohr exciton. Addition of 3d transition-metal ions impurities in semiconductors form deep levels states within the band gaps of the host materials [14].

Semiconductors are also utilized as photosensitizers, where optical excitation creates an electron and hole concentration which may then react with adsorbed molecular species. The question naturally arises as to the correct physical description of the confined electron and hole, i.e., as to the nature of the crystallite excited electronic states. This question in turn depends intimately upon the actual structure and size of the aggregate [15]. They are technologically important as luminescence centers and charge compensations as well as unwanted traps. Efficient photocatalytic processes have been proven to be of a great contribution in treatment of environmental deprivation. Photocatalytic oxidation of organic and biological molecules is one of the most efficient methods for alleviating the negative environmental impact of hazardous wastes and toxic pollutants in aqueous media [6, 12]. The superiority of photocatalytic technique in wastewater treatment is due to its advantages over the traditional techniques such as quick oxidation, high efficiency, no formation of polycyclic products and oxidation of pollutants in the low levels [16].

Yang et al [17] examined strong visible-light emitting (with a color range from blue to green) ZnS nanoparticles co-doped with $Ni^{2+}$ and $Mn^{2+}$ The emission peak of un-doped ZnS nanoparticles is at 450 nm ($\lambda_{ex}$ = 308 nm). The emission peak of the $Ni^{2+}$-doped ZnS nanoparticles is at 520 nm ($\lambda_{ex}$ = 310 nm). The emission peak of the ZnS nanoparticles co-doped with $Ni^{2+}$ and $Mn^{2+}$ is at 475–540 nm and their fluorescence intensity is remarkably elevated than that of un-doped ZnS nanocrystals. A novel PL

*Corresponding Author:velusubhash@gmail.com(S. Velusubhash)

https://doi.org/10.30799/jnst.143.18040501


*Cite this Article as:* S. Velusubhash, K. Kalirajan, S. Harikengaram, R. Vettumperumal, R. Murugesan, A. Rajarajeswari, Influence of co-dopant on structural, optical and electrochemical properties of zinc sulphide quantum dots, J. Nanosci. Tech. 4(5) (2018) 461–466.

phenomenon can be detected from the ZnS nanocrystallites co-doped with $Ni^{2+}$ and $Mn^{2+}$ ions.

Ashkarran [18] reported XRD results of Mn doped ZnS NPs which indicated the formation of zinc blend phase and the mean particle size was found to be between 4 and 6 nm according to TEM analysis. Further, the PL study of Mn doped ZnS NPs established a broad emission peak around 600 nm. In addition this test revealed that the 7.5% Mn doped ZnS NPs have the most intensive PL peak among all doped and un-doped samples. Photocatalytic performance of Mn doped ZnS NPs was explored in the presence of 3 different dyes and the results revealed that unlike the PL results not only was there a remarkable difference in photocatalytic performance of Mn doped ZnS NPs but also photocatalytic activity was decreased by Mn doping and the photocatalytic activity was absent where the PL was present.

Divya et al [19] found that ZnS nanoparticles co-doped with Mn and Te ($x$ = 0.05 and 0.10) Particle sizes was in the range of 3 – 5 nm were obtained with cubic zinc-blende phase. The samples showed photoluminescence in the red region with composition dependent emission wavelength. The intensity of emission decreases with increasing dopant concentration of Mn and Te.

Crafting materials with specific band gaps belongs to the area termed band gap engineering. As part of this work, we have analysed ZnS QDs with specific goals of band gap modification. By incorporating Co and Ni metal ions into ZnS crystal lattice, we have established and discussed very useful mechanisms for band gap reduction. In this study, undoped ZnS QDs (ZnS QDs), Co-3% doped ZnS QDs (ZnS: Co(3%) QDs), Co-3% doped and Ni-1% co-doped ZnS QDs (ZnS : Co(3%), Ni(1%) QDs) and Co-3% doped and Ni-5% co-doped co-doped ZnS QDs (ZnS : Co(3%), Ni(5%) QDs) were prepared by simple chemical precipitation technique. The structural, surface morphological, optical properties and electrochemical properties of the prepared ZnS QDs samples were characterized by X-ray diffraction studies (XRD), scanning electron microscopy (SEM) along with EDX, UV-visible spectroscopy (UV-vis), photoluminescence (PL), electrochemcial impedance spectroscopy (EIS) study and photocatalytic degradation.

## 2. Experimental Methods

### *2.1 Materials*

Zinc acetate dehydrate ($Zn(CH_3COO)_2.2H_2O$), nickel chloride (II) hexa hydrate ($NiCl_2.6H_2O$), cobalt (II) chloride hexa hydrate ($CoCl_2.6H_2O$), sodium sulphide ($Na_2S$) were purchased from Hi-Media, India with high purity (99.99%), Water was used after two distillations (DDW).

### *2.2 Synthesis*

ZnS QDs, ZnS: Co(3%) QDs ($Zn_{0.97-x}Co_{0.03}Ni_x$ (x=0)), ZnS : Co(3%), Ni(1%) QDs ($Zn_{0.97-x}Co_{0.03}Ni_x$ (x=1%)), ZnS : Co(3%), Ni(5%) QDs ($Zn_{0.97-x}Co_{0.03}Ni_x$ (x=5%)) were synthesized by chemical precipitation method.

#### *2.2.1 Synthesis of ZnS Hybrid QDs*

ZnS QDs were prepared by chemical precipitation method. In a typical procedure, 2 M of $Zn(CH_3COO)_2.2H_2O$ in 50 mL of deionized water and an equal molar concentration of sodium sulphide in deionized water were mixed drop by drop. The solution was heated about 80 °C temperature under constant magnetic stirring for 2 hours. The obtained precipitate was collected and washed several times with deionized water and ethanol and centrifuged. The precipitate was dried in a hot air oven at 120 °C for 6 hours, ground to obtain ZnS QDs.

The $Zn_{0.97-x}Co_{0.03}Ni_x$ (x= 0, 0.01, 0.05, x at %) samples were prepared according to the following procedure.

#### *2.2.2 Preparation of Co (3%) Doped ZnS ($Zn_{0.97-x}Co_{0.03}Ni_x$ (x=0))*

Co (3%) doped ZnS QDs samples were prepared by chemical precipitation method. 1.94 M $Zn(CH_3COO)_2.2H_2O$ and 0.06 M $CoCl_2.6H_2O$ were dissolved (Zn:Co =0.97:0.03, in mol) in 50 mL of distilled water, stirred for 10 min. And then 2 M sodium sulfide aqueous solution was added to the above solution mixture drop-by-drop under constant magnetic stirring. The solution was heated about 80 °C temperature under continued stirring for 2 hours. The obtained precipitate was washed with de-ionised water and ethanol for several times and centrifuged. The precipitate was dried for 6 hours at 120 °C and ground to obtain Co (3%) doped ZnS QDs sample.

#### *2.2.3 Preparation of Co (3%) Doped and Ni(1%) Co-Doped ZnS QDs ($Zn_{0.97-x}Co_{0.03}Ni_x$ (x=1))*

Co (3%) and Ni (1%) co- doped ZnS QDs sample were prepared by chemical precipitation method. 1.92 M $Zn(CH_3COO)_2.2H_2O$ in 50 mL of distilled water, 0.06 M $CoCl_2.6H_2O$ and 0.02 M $NiCl_2.6H_2O$ were dissolved (Zn:Co:Ni =0.96:0.03:0.01, in mol) in 50 mL of distilled water stirred for 10 min. And then 2 M sodium sulfide aqueous solution was added to the above solution mixture drop-by-drop under constant magnetic stirring. The solution was heated about 80 °C temperature under continued stirring for 2 hours. The obtained precipitate was washed with de-ionised water and ethanol for several times and centrifuged. The precipitate was dried for 6 hours at 120 °C and ground to obtain Co (3%) and Ni (1%) co- doped ZnS QDs sample.

#### *2.2.4 Preparation of Co (3 %) Doped and Ni (5 %) Co-Doped ZnS QDs ($Zn_{0.97-x}Co_{0.03}Ni_x$ (x=5))*

Co (3%) and Ni (1%) co- doped ZnS QDs sample were prepared by chemical precipitation method. 1.84 M $Zn(CH_3COO)_2.2H_2O$ and 0.06 M $CoCl_2.6H_2O$ and 0.10 M $NiCl_2.6H_2O$ were dissolved (Zn:Co:Ni =0.92:0.03:0.05, in mol) in 50 mL of distilled water and stirred for 10 min. And then 2 M Sodium sulfide aqueous solution was added to the above solution mixture drop-by-drop under constant magnetic stirring was heated about 80°C temperature under continued stirring for 2 hours. The obtained precipitate was washed with de-ionised water and ethanol for several times and centrifuged. The precipitate was dried for 6 hours at 120 °C and ground to obtain to obtain Co (3%) and Ni (5%) co- doped ZnS QDs sample.

### *2.3 Characterization Techniques*

XRD 6000 X-ray diffraction with Cu-Kα radiation source (λ=1.54 Å) operated at 40 kV and 30 mA in the 2θ range 10-90° at the scan speed of 10.0° per minute. Surface morphological and elemental analysis of prepared samples was done by using scanning electron microscope (SEM; JSM 6390, JEOL, USA) equipped with energy dispersive X-ray analysis spectrometer (EDAX; INCA, Oxford). The obtained nanopowders have been dissolved in ethanol through sonication, and their optical absorption spectra have been recorded with the help of Uv-vis spectrophotometer (Shimadzu model) at room temperature over the range of 200 to 800 nm. Photoluminescence (PL) measurements were performed at room temperature in JASCO FP-8200 spectrofluorometer. The samples were dispersed in ethanol solvent, excited with excitation wavelengths of 330 nm and the spectra were recorded ranging from 300 nm to 900 nm. The electrochemical experiments were carried out to measure electrochemical impedance was conducted with an electrochemical system (CH-Instrument Inc., TX, USA, mod 650C). Visible light was obtained from a 200 W Tungsten lamp.

### *2.4 Electrochemical Studies*

To investigate the transition of photogenerated electrons in ZnS QDs, ZnS: Co(3%) QDs, ZnS: Co(3%), Ni(1%) QDs, ZnS: Co(3%), Ni(5%) QDs modified electrodes comprising the prepared QDs samples were prepared. The electrochemical impedance was measured with an electrochemical workstation (mode 650C, CH-Instrument Inc., TX, USA). It consist of a standard three-electrode system, platinum wire act as counter electrode, Silver/Silver chloride electrode as reference electrode, and a Glassy carbon electrode (GCE) as working electrode, respectively. A 200 W tungsten lamp was utilized as the light source. A 0.1 M $Na_2SO_4$ aqueous solution was used as the electrolyte. The ZnS QDs modified electrode was prepared by a simple casting method as follows: 5 µL ZnS QDs sample suspension was dropped onto the pretreated GCE and dried in air at room temperature. Similarly all other samples casted GCE were prepared. The Nyquist plots were recorded the 1 MHz to 1 kHz frequency range.

### *2.5 Photocatalytic Procedure for the Removal of Malachite Green*

Photocatalytic activity of the as prepared samples was evaluated by the degradation of MG under 200 W Tungsten lamps. 0.04 g photocatalysts were added in 100 mL MG (10 $mgL^{-1}$) in a 500 mL glass beaker. Afterward, the suspensions were magnetically stirred for 30 min in the dark to ensure that the MG could reach the absorption–desorption equilibrium, The irradiation was carried out with a 200 W Tungsten lamp, which was put above beaker. The distance between the solution and lamp was constant, 15 cm, in all experiments with maximum illumination time up to 120 min. At regular time intervals, 2 mL of the samples was taken and was analyzed, by using UV-visible spectrophotometer (Agilent 8453 UV-Vis spectrophotometer, USA) at the maximal absorption wavelength of MG whose characteristic absorption peak was chosen to be 618 nm. The decrease in the absorbance value of the malachite green dye samples after irradiation in a definite time interval is a measure of the presence of dye and its removal rate, as well as the photocatalytic activity of the prepared QDs. Furthermore, all experiments were performed at room temperature under constant stirring.

https://doi.org/10.30799/jnst.143.18040501

*Cite this Article as:* S. Velusubhash, K. Kalirajan, S. Harikengaram, R. Vettumperumal, R. Murugesan, A. Rajarajeswari, Influence of co-dopant on structural, optical and electrochemical properties of zinc sulphide quantum dots, J. Nanosci. Tech. 4(5) (2018) 461–466.

## 3. Results and Discussion

### *3.1 XRD Studies*

X–ray diffraction patterns of the prepared samples are shown in Fig. 1. The peak position confirms that the particles exhibit a cubic zinc blende crystal structure. The three diffraction peaks is appearing at about 29°, 48°, and 56° in all the samples corresponds to the most preferred orientation namely (111), (220) and (311) of cubic zinc blende crystallites ZnS (JCPDS No: 05 –0566) [20]. The addition of dopant and co-dopants alters the peak position and intensity. The well broaden peak width indicates the formation of nanocrystallites in the samples. The average crystalline sizes were calculated from the full width and half maximum of diffraction peaks using Debye Scherrer's formula [21],

$$D = 0.94\lambda / \beta \cos\theta \qquad (1)$$

where D is the crystallite size, λ is the wavelength of Cu $K_\alpha$ radiation and β is full width at half maximum (FWHM) after correcting the instrument peak broadening (β expressed in radians). All samples exhibit crystallite size in the range of 1.4 to 1 nm. Particle size increases as the number of dopant and variation of concentration of dopants (Co and Ni) increases. It is found that at 5% Ni concentration particles size increases. XRD broadening could be also due to contributions of strain (ε). Hence an attempt has been made to estimate the average strain of the as prepared ZnS QDs samples using Stokes-Wilson equation (Eq.(2)) [22] and the values are tabulated in Table 1.

$$\text{Strain} = \beta / 4\tan\theta \qquad (2)$$

The doping makes distortion in the host lattice which can be seen in the variation of strain calculated from the above formula.

**Table 1** Particle size and strain of the ZnS QDs, ZnS: Co(3%) QDs, ZnS: Co(3%), Ni(1%) QDs, ZnS: Co(3%), Ni(5%) QDs

| S.No | Sample | Particle size (nm) | Strain |
|---|---|---|---|
| 1 | ZnS QDs | 1 | 0.09771859 |
| 2 | ZnS:Co (3%) QDs | 1.2 | 0.10696063 |
| 3 | ZnS:Co (3%): Ni(1%) QDs | 1.3 | 0.11308541 |
| 4 | ZnS:Co(3%):Ni (5%) QDs | 1.4 | 0.13546658 |

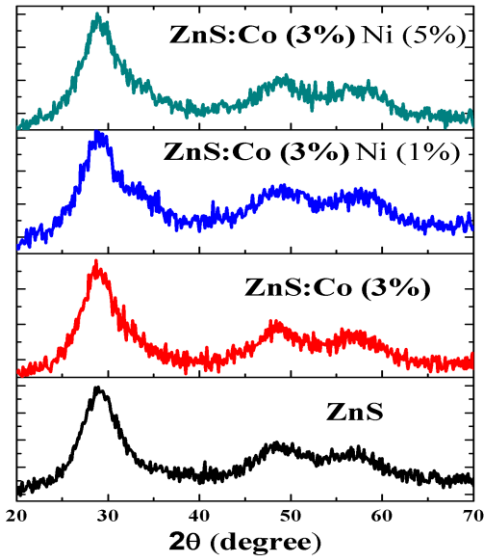


**Fig. 1** XRD Pattern of ZnS QDs, ZnS: Co(3%) QDs, ZnS: Co(3%), Ni(1%) QDs, ZnS: Co(3%), Ni(5%) QDs

### *3.2 Morphological and Compositional Analysis*

Fig. 2(a-d) shows the SEM images of ZnS QDs, ZnS: Co(3%) QDs, ZnS: Co(3%), Ni(1%) QDs, ZnS: Co(3%), Ni(5%) QDs. It is clearly observed that the agglomeration level is altered in the co-doped ZnS: Co, Ni samples compared to undoped samples. Co doped ZnS QDs have flakes like structure and Co and Ni Co-doped ZnS QDs has been modified to spherical morphology. Thus co-doped ZnS: Co, Ni samples has immense effect on the surface morphology of QDs showing fine distribution and decrease the particle size. The compositions of the samples were examined using an energy-dispersive X-ray (EDAX) spectroscopy analysis. The EDAX analysis from Fig. 3 demonstrated that Zn, Co, Ni and S elements are present in the sample which further confirmed the successful doping of Co and Ni ions in the ZnS host structure.

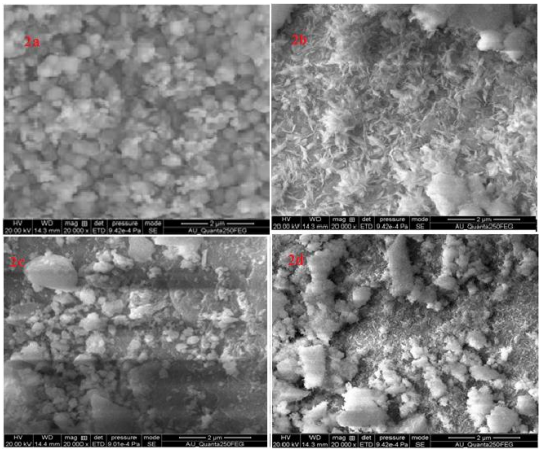


**Fig. 2** a) SEM image of ZnS QDs, b) SEM image of Co (3%)-doped ZnS , c) SEM image of Co(3%) Ni (5%) co-doped ZnS QDs, d) SEM image of Co (3%) Ni (5%) co-doped ZnS QDs

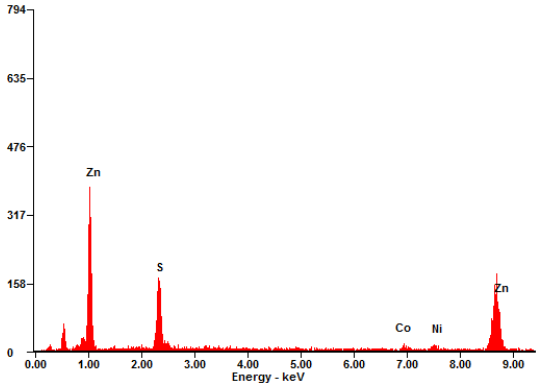


**Fig. 3** EDX pattern of co-doped ZnS:Co,Ni QDs

### *3.3 Optical study*

#### *3.3.1 UV-Visible Studies*

Fig. 4 shows the UV–vis absorption spectra of ZnS QDs, ZnS: Co(3%) QDs, ZnS: Co(3%), Ni(1%) QDs, ZnS: Co(3%), Ni(5%) QDs. For all the samples broad absorption edge appears between 297 nm and 306 nm. These are blue shifted compared to bulk adsorption edge (338 nm) [21]. The blue shift of the absorption edge is due to the quantum confinement effect caused by the photo-generated electron–hole pairs.

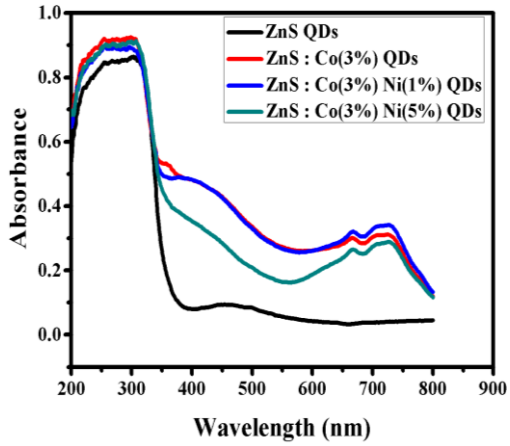


**Fig. 4** Optical absorbance spectra for ZnS QDs, ZnS: Co(3%) QDs, ZnS: Co(3%), Ni(1%) QDs, ZnS: Co(3%), Ni(5%) QDs

The estimated band gap for all the samples are calculated using the following Eq.(3) [23],

$$(\alpha h\nu)^2 = A(h\nu - E_g)^n \qquad (3)$$

where h is the Plank's constant, ν is the photo-frequency, A is a constant, Eg is the band-gap and n is the index which depends on the type of transition. The n value for a direct band-gap semiconductor is 1/2, and is 2 for an indirect band-gap semiconductor. ZnS is a direct band-gap semiconductor, therefore n=1/2 [23]. Thus, the estimated band-gap can be

https://doi.org/10.30799/jnst.143.18040501

obtained from the plot of $(\alpha h\nu)^2$ vs hν as shown in the Fig. 5 and tabulated in Table 2. The band gap of the undoped ZnS is 3.7 eV and for Co-doped ZnS it is found to be 3.68. Band gap for 1% Ni and 5% Ni is 3.65 eV and 3.60 eV respectively. It is observed that the band gap decreases as doping and co-doping of metal ions interact with ZnS QDs. Generally, the band-gap value increases with the decreases in the particle size and vice-versa [21].

**Table 2** Absorbance and Band gap ZnS QDs, ZnS: Co(3%) QDs, ZnS: Co(3%), Ni(1%) QDs, ZnS: Co(3%), Ni(5%) QDs

| S.No | Sample | Absorbance (nm) | Band gap |
|---|---|---|---|
| 1 | ZnS QDs | 296 | 3.7 |
| 2 | ZnS:Co (3%) | 299 | 3.68 |
| 3 | ZnS:Co(3%): Ni(1%) | 303 | 3.65 |
| 4 | ZnS:Co(3%):Ni (5%) | 307 | 3.6 |

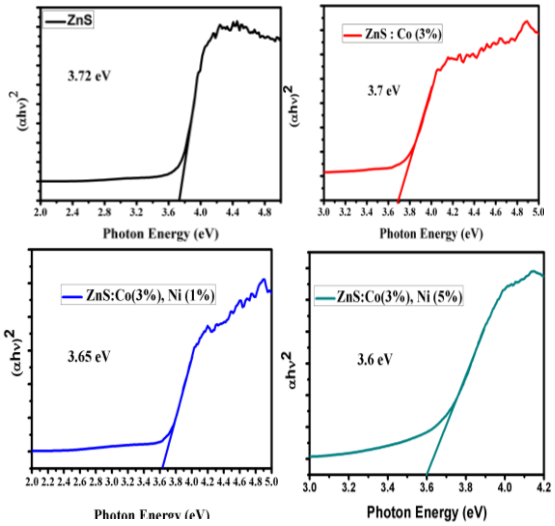


**Fig. 5** Plot of $(\alpha h\nu)^2$ versus photon energy of ZnS QDs, ZnS: Co(3%) QDs, ZnS: Co(3%), Ni(1%) QDs, ZnS: Co(3%), Ni(5%) QDs

The absorption band edge is also found at the range of 400 to 440 nm and in 650 to 730 nm, which indicates that QDs responds to visible light for photocatalytic reaction. Doped and co-doped samples exhibited enhanced absorption capability especially in the visible light region mentioned above compared to undoped ZnS samples. Hence effective enhancement in photoabsorption capacity in visible region takes place for doped and co-doped QDs samples which in turn leading to a higher absorption capability. Therefore, Co and Ni metal ion act as sensitizer and effectively increases the visible light absorption capacity of ZnS QDs. The modified absorption property of Co-doped and Ni co-doped samples would probably improve the photocatalytic activity of ZnS QDs.

### *3.3.2 PL Study*

Photoluminescence spectra of ZnS QDs, ZnS: Co(3%) QDs, ZnS: Co(3%), Ni(1%) QDs, ZnS: Co (3%), Ni(5%) QDs excited using a wavelength of 330 nm. The emission band at 658.5 nm was noticed for all the prepare QDs. Fig 6. Shows the intensity of Photoluminescence emission was observed to decrease with inclusion of Co dopant and Ni co-dopant and corresponding peak wavelength and intensity are tabulated in Table 3. This implies that the quenching would have taken place in ZnS QDs because of the interaction with Co dopant and Ni do-dopant. Red emission is because of transition between deep level states formed due to dopant and co-dopant [23].

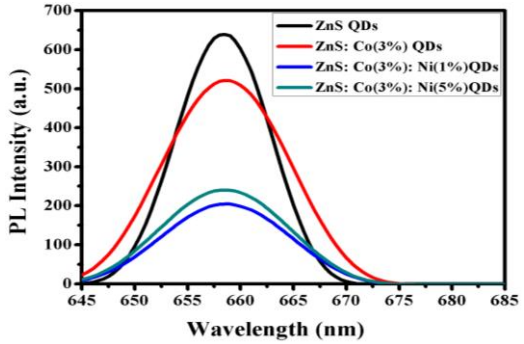


**Fig. 6** Photoluminescence spectra of ZnS QDs, ZnS: Co(3%) QDs, ZnS: Co(3%), Ni(1%) QDs, ZnS: Co(3%), Ni(5%) QDs

**Table 3** PL Peak wavelength and Intensity

| S.No | Sample | Peak (nm) | Peak Intensity |
|---|---|---|---|
| 1 | ZnS QDs | 658.5 | 639 |
| 2 | ZnS: Co(3%) QDs | 658.5 | 521 |
| 3 | Co(3%), Ni(1%) QDs | 658.5 | 241 |
| 4 | Co(3%), Ni(5%) QDs | 658.5 | 204 |

### *3.4 Electrochemical Study*

To make a better sense for the role of ZnS QDs, ZnS doped Co (3%) QDs, ZnS doped Co (3%) co-doped Ni (1 %) QDs ZnS doped Co (3%) co-doped Ni (5 %) QD in photocatalytic degradation, Nyquist plots obtained through electrochemical impedance spectroscopy (EIS) were discussed. As shown in Fig. 7, the Nyquist impedance plots for ZnS QDs, ZnS doped Co (3%) QDs, ZnS doped Co (3%) co-doped Ni (1 %) QDs ZnS doped Co (3%) co-doped Ni (5 %) QD electrode materials cycled in 0.1 M $Na_2SO_4$ electrolyte solution exhibit semicircles at high frequencies with irradiation. The arc radius of the EIS Nyquist plot of co-doped samples are found to be smaller than that of rest of the samples in presence of radiation, suggesting that doping and co-doping by Co and Ni metal ions changes the charge distribution of ZnS QDs and makes charge transfer easier [24]. A smaller arc radius of the EIS Nyquist plot of doped and co-doped samples under visible-light irradiation is also observed, indicating a more effective separation efficiency of photogenerated electron–hole pairs and a faster interfacial charge transfer [25].

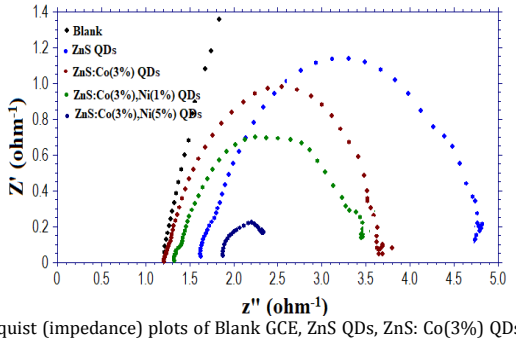


**Fig. 7** Nyquist (impedance) plots of Blank GCE, ZnS QDs, ZnS: Co(3%) QDs, ZnS: Co (3%), Ni(1%) QDs, ZnS: Co (3%), Ni (5%) QDs

This result implies that the doping and co-doping has brought a change in the electrochemical behaviour of ZnS QDs. Thus inclusion of dopant and co-dopant into the ZnS lattice will increase the photocatalytic activity. ZnS: Co(3%), Ni(5%) QDs has found to have minimum charge transfer resistance which leads to effective photocatalysis reaction.

### *3.5 Photocatalytic Studies*

Photocatalytic experiments were carried out with an initial concentration of MG was taken as 10 mg/L, catalyst concentration of 400mg/L, irradiation time of 120 min. The photocatalytic activity of as prepared undoped, mono doped and double doped ZnS QDs was studied for reference. Fig. 8 shows the change in absorption spectra of MG exposed to visible light for various irradiation times (0 min, 30 min, 60 min, 90 min and 120 min) in the presence of as prepared samples. The absorption maxima at 618 nm decreased gradually with time. The comparison of photodegradation removal percentage of MG when mixed with ZnS QDs, ZnS : Co(3%) QDs, ZnS : Co(3%), Ni(1%) QDs, ZnS : Co(3%), Ni(5%) QDs are shown in Fig. 9. In order to evaluate the photocatalytic performance, the degradation rate (D) can be calculated from the following Eq.(4) [26],

$$D = \frac{C_o - C_t}{C_o} X\ 100\ \% = \frac{A_o - A}{A} X\ 100\% \qquad (4)$$

where $C_o$ is the initial concentration of Malachite green (10 mg/L). $C_t$ is the concentration after t min of photocatalytic degradation. $A_o$ is the initial absorbance corresponding to initial concentration of malachite green dye. $A_t$ is the absorbance after time t min of photocatalytic degradation. Fig. 8 shows Absorption spectra of MG dye under visible radiation in presence of prepared nano photocatalyst.

The results displayed in Table 4 revealed that the mono doped and double doped showed higher photocatalytic activity than that of bare ZnS QDs. They showed remarkable photo-catalytic activity with a degradation of 93% and 95% for MG respectively. The increase percentage of dye degradation confirms the mineralization of MG during photodegradation. Therefore, doping of Co along with Ni in ZnS QDs significantly improves its photocatalytic activity by enhancing the electron–hole separation on the photocatalyst surface. Photo-catalytic activity degradation of ZnS QDs and Co doped ZnS QDs was found to be 75% and 85% respectively.

https://doi.org/10.30799/jnst.143.18040501

*Cite this Article as:* S. Velusubhash, K. Kalirajan, S. Harikengaram, R. Vettumperumal, R. Murugesan, A. Rajarajeswari, Influence of co-dopant on structural, optical and electrochemical properties of zinc sulphide quantum dots, J. Nanosci. Tech. 4(5) (2018) 461–466.

The photocatalyst represents positive effect with the inclusion of dopant and co-dopant into the ZnS lattice. This behavior is explained based on the charge carrier trapping. As far as prepared samples are concerned, $Co^{+2}$ and $Ni^{2+}$ serves as trap state for ZnS. When the charge carriers are generated under visible light irradiation, there exist a competition between charge carrier recombination and charge carrier trapping, followed by competition between recombination of trapped carriers and interfacial charge transfer [27]. For efficient photodegradation, the charge carrier trapping, followed by interfacial charge transfer should predominate the charge carrier recombination. Exactly, the same condition is followed when the Co and Ni is doped into the ZnS crystal lattice.

During the photocatalytic process, the incident photons excite the valence band electrons of the photocatalyst to the conduction band, thus generating electron–hole pairs. The dissolved $O_2$ molecules in the suspension capture the electron in the conduction band. The $H_2O$ molecules are adsorbed on the surface of the catalyst and interact with the generated valence band hole to produce the $^{*}OH$ radicals, which subsequently participate in the oxidation. A possible mechanism has also been to explain the effects of Co and Ni dopants on the photocatalytic performance of ZnS QDs. Under visible light irradiation, the electrons can be promoted from the valence band to the conduction band or the impurity level. The existence of $Co^{2+}$ and $Ni^{2+}$ dopant within the crystal matrix or on the surface of ZnS QDs samples can trap photogenerated electrons or holes and subsequently transfer the same to adsorbed oxygen and hydroxyl ions to generate super oxide radicals ($O_2^{*-}$) and hydroxide radicals (*OH), respectively [28]. These processes effectively suppress the electron–hole recombination and give rise to excess free radicals necessary for the degradation of MG. Therefore, the photocatalytic activity of mono and double doped ZnS is greatly improved.

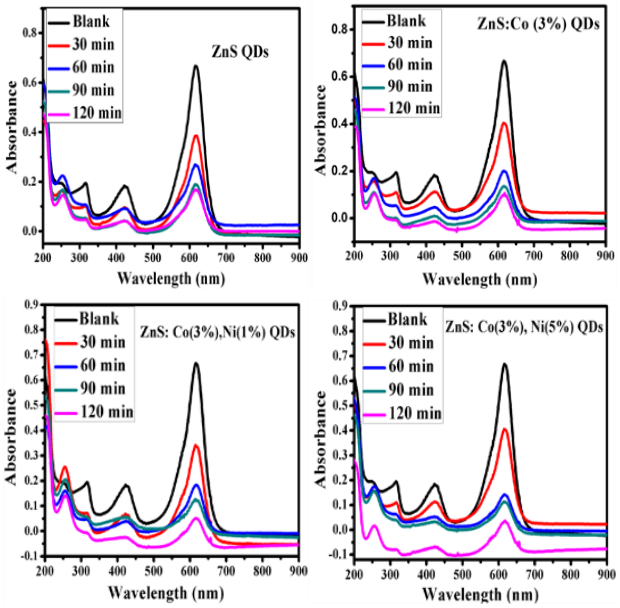


*Condition: [MG Dye] =10 mg/L, Catalyst dose=0.4 mg/L, Temperature- 28 °C*

**Fig. 8** Absorption spectra of MG dye under visible radiation indicating their degradation in presence of a) ZnS QDs, b) ZnS : Co(3%) QDs, c) ZnS : Co(3%), Ni(1%) QDs, d) ZnS : Co(3%), Ni(5%) QDs

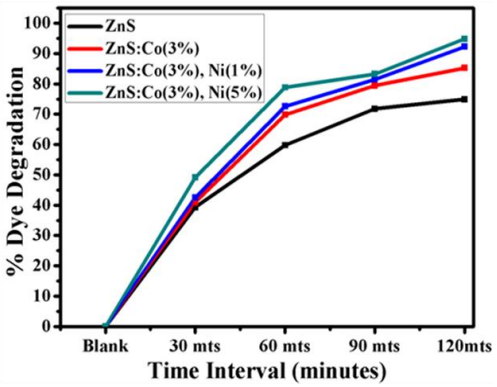


**Fig. 9** Effect of time on MG dye degradation in presence of ZnS QDs, ZnS : Co(3%) QDs, ZnS : Co(3%), Ni(1%) QDs, ZnS : Co(3%), Ni(5%) QDs

**Table 4** Percentage Dye degradation of with ZnS QDs, ZnS : Co(3%) QDs, ZnS : Co(3%), Ni(1%) QDs, ZnS : Co(3%), Ni(5%) QDs

| S.No | Name of the sample | % Dye Degration |
|---|---|---|
| 1 | ZnS QDs | 75 |
| 2 | ZnS : Co(3%) QDs | 85 |
| 3 | ZnS : Co(3%), Ni(1%) QDs | 93 |
| 4 | ZnS : Co(3%), Ni(5%) QDs | 95 |

## 4. Conclusion

ZnS nanoparticles co-doped with Co and Ni were obtained by precipitation from homogeneous solutions of zinc, Cobalt and Nickel salt compounds, with $S^{2-}$ as precipitating anion from $Na_2S$. XRD studies reveal the zinc blende structure for the all the synthesized samples with particle size in the range of QDs. SEM images confirm the co-doping technology by screening difference in surface morphology of Co doped ZnS QDs and Co, Ni co-doped zinc sulphide QDs. The optical absorption spectra of undoped, doped and Co-doped ZnS QDs shows that the absorption edge is observed around 297-306 nm, which is blue shifted when compared to that of bulk ZnS (345 nm) and indicates the presence of quantum size confinement. The PL spectra show strong visible emission (with a color range from violet to red) for the prepared ZnS QDs samples at room temperature. All the peak intensities vary with the addition of dopant and co-dopant. EIS studies indicated that QDs samples exhibited as a superior electrochemical catalyst which acts as supporting evidence to the increase in photo catalytic activity due to the incorporation of dopant and co-dopant in to the ZnS QDs lattice.

## References

[1] M. Bangal, S. Ashtaputer, S. Marathe, A. Ethiraj, N. Hebalkar, S.W. Gosavi, S.K. Kulkarni, Semiconductor nanoparticles, Hyperfine Interact. 160 (2005) 81-94.
[2] U.K. Gautam, X. Fang, Y. Bando, J. Zhan, D. Golberg, Synthesis, structure and multiply enhanced field-emission properties of branched ZnS nanotube-in nanowire core-shell heterostructures, ACS Nano 2 (2008) 1015-1021.
[3] M.L. Breen, A.D. Dinsmore, R.H. Pink, S.B. Qadri, A.B. Ratna, Sonochemically produced ZnS-coated polystyrene core-shell particles for use in photonic crystals, Langmuir 17 (2001) 903-907.
[4] X. Fang, Y. Bando, M. Liao, U.K. Gautam, C. Zhi, B. Dierre, D. Golberg, Single crystalline ZnS nanobelts as ultraviolet light sensors, Adv. Mater. 21 (2009) 2034-2039.
[5] K.T. Yong, I. Roy, M.T. Swihart, P.N. Prasad, Multifunctional nanoparticles as biocompatible targeted probes for human cancer diagnosis and therapy, J. Mater. Chem. 19 (2009) 4655-4672.
[6] H. Labiadh, K. Lahbib, S. Hidouri, S. Touil, T.B. Chaabane, Insight of ZnS nanoparticles contribution in different biological uses, Asian Pac. J. Trop. Med. 9 (2016) 757-762.
[7] M. Han, X. Gao, J.Z. Su, S. Nie, Quantum-dot-tagged microbeads for multiplexed optical coding of biomolecules, Nat. Biotechnol. 19 (2001) 631-635.
[8] S. Biswas, S. Kar, S. Chaudhuri, Optical and magnetic properties of manganese-incorporated zinc sulfide nanorods synthesized by a solvothermal process, J. Phys. Chem. B. 109 (2005) 17526-17530.
[9] C. Lü, Z. Cui, Y. Wang, Z. Li, C. Guan, B. Yang, J. Shen, Preparation and characterization of ZnS-polymer nanocomposite films with high refractive index, J. Mater. chem. 13 (2003) 2189-2195.
[10] N. Saravanan, G.B. Teh, S.Y.P. Yap, K.M. Cheong, Simple synthesis of ZnS nanoparticles in alkaline medium, J. Mater. Sci-Mater. El. 19 (2008) 1206-1208.
[11] I.P. McClean, C.B. Thomas, Photoluminescence study of MBE-grown films on ZnS, Semicond. Sci. Technol. 7 (1992) 1394-1399.
[12] N. Soltani, E. Saion, W.M.M. Yunus, M. Erfani, M. Navasery, G. Bahmanrokh, K. Rezaee, Enhancement of visible light photocatalytic activity of ZnS and CdS nanoparticles based on organic and inorganic coating, Appl. Surf. Sci. 290 (2014) 440-447.
[13] J. Chang, E.R. Waclawik, Colloidal semiconductor nanocrystals: controlled synthesis and surface chemistry in organic media, RSC Adv. 4 (2014) 3505-23527.
[14] G. Murugadoss, B. Rajamannan, V. Ramasamy, G. Viruthagiri, Synthesis and characterization of Mn2+-doped ZnS luminescent nanocrystals, J. Ovonic. Res. 5 (2009) 107-116.
[15] R. Rossetti, J.L. Ellison, J.M. Gibson, L.E. Brus, Size effects in the excited electronic states of small colloidal CdS crystallites, J. Chem. Phys. 80 (1984) 4464-4469.
[16] W.C. Liu, H.Y. Xu, T.N. Shi, L.C. Wu, P. Li, Preparation and photocatalytic activity of $TiO_2$/tourmaline composite catalyst, Adv. Mat. Res. 800 (2013) 464-470.
[17] H. Yang, P.H. Holloway, B. Ratna, Photoluminescent and electroluminescent properties of Mn-doped ZnS nanocrystals, J. Appl. Phys. 93 (2003) 586-592.
[18] A.A. Ashkarran, Absence of photocatalytic activity in the presence of the photoluminescence property of Mn–ZnS nanoparticles prepared by a facile wet chemical method at room temperature, Mater. Sci. Semicond. Process. 17 (2014) 1-6.
[19] A. Divya, B.K. Reddy, S. Sambasivam, P.S. Reddy, Photoluminescence and EPR studies of ZnS nanoparticles Co-Doped with Mn and Te, J. Nano-Electron. Phys. 3 (2011) 639-646.
[20] R.K. Srivastava, N. Pandey, S.K. Mishra, Effect of Cu concentration on the photoconductivity properties of ZnS nanoparticles synthesized by co-precipitation method, Mater. Sci. Semicond. Process. 16 (2013) 1659 - 1664.

https://doi.org/10.30799/jnst.143.18040501

*Cite this Article as:* S. Velusubhash, K. Kalirajan, S. Harikengaram, R. Vettumperumal, R. Murugesan, A. Rajarajeswari, Influence of co-dopant on structural, optical and electrochemical properties of zinc sulphide quantum dots, J. Nanosci. Tech. 4(5) (2018) 461–466.

[21] D.A. Reddy, S. Sambasivam, G. Murali, B. Poornaprakash, R.P. Vijayalakshmi, Y. Aparna, J.L. Rao, Effect of Mn co-doping on the structural, optical and magnetic properties of ZnS: Cr nanoparticles, J. Alloys. Compd. 537 (2012) 208-215.
[22] M.S. Al-Kotb, J.Z. Al-Waheidi, M.F. Kotkata, Investigation on microstructural and optical properties of nano-crystalline CdSe thin films, Thin Solid Films 631 (2017) 219-226.
[23] M. Sookhakian, Y.M. Amin, W.J. Basirun, M.T. Tajabadi, N. Kamarulzaman, Synthesis, structural, and optical properties of type-II ZnO–ZnS core–shell nanostructure, J. Lumin. 145 (2014) 244-252.
[24] Y. Zhang, R. Wen, D. Guo, H. Guo, J. Chen, Z. Zheng, One-step facile fabrication and photocatalytic activities of ZnS@ g-$C_3N_4$ nanocomposites from sulfatotris (thiourea) zinc (II) complex, Appl. Organomet. Chem. 30 (2016) 160-166.
[25] Y. Li, X. He, M. Cao, Micro-emulsion-assisted synthesis of ZnS nanospheres and their photocatalytic activity, Mater. Res. Bull. 43 (2008) 3100-3110.
[26] J.H. Xiao, W.Q. Huang, Y.S. Hu, F. Zeng, Q.Y. Huang, B.X. Zhou, G.F. Huang, Facile in situ synthesis of wurtzite ZnS/ZnO core/shell heterostructure with highly efficient visible-light photocatalytic activity and photostability, J. Phys. D: Appl. Phys. 51 (2018) 1-26.
[27] M. Chitkara, K. Singh, I.S. Sandhu, H.S. Bhatti, Photo-catalytic activity of $Zn_{1-x}Mn_xS$ nanocrystals synthesized by wet chemical technique, Nanoscale Res. Lett. 6 (2011) 438-442.
[28] S.S. Boxi, S. Paria, Effect of silver doping on $TiO_2$, CdS, and ZnS nanoparticles for the photocatalytic degradation of metronidazole under visible light, RSC Adv. 4 (2014) 37752-37760.

https://doi.org/10.30799/jnst.143.18040501

*Cite this Article as:* S. Velusubhash, K. Kalirajan, S. Harikengaram, R. Vettumperumal, R. Murugesan, A. Rajarajeswari, Influence of co-dopant on structural, optical and electrochemical properties of zinc sulphide quantum dots, J. Nanosci. Tech. 4(5) (2018) 461–466.